

Thermal Polymerization of Styrene

A. HUSAIN and A. E. HAMIELEC, *McMaster University, Hamilton, Ontario, Canada L8S 4L7*

Synopsis

An experimental investigation of the kinetics of bulk thermal polymerization of styrene in the temperature range of 200°–230°C is reported. Conversions and molecular weight averages were measured by gel permeation chromatography. At elevated temperatures, oxygen in the polymerization mixture appears to have negligible effect on the rate of polymerization and the molecular weights of the polymer. Experimental evidence suggests that the molecular weight development of the polymer is strongly influenced by transfer reactions.

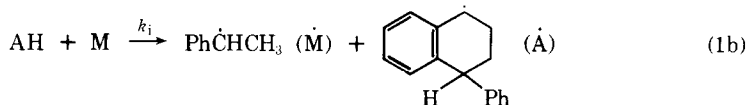
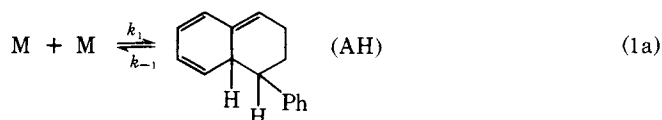
INTRODUCTION

Styrene is one of the few vinyl monomers that undergo rapid thermal polymerization. Bulk thermal polymerization of styrene is, therefore, a common method for industrial polystyrene manufacture. The industrial process involves polymerizing the monomer to high conversions at temperatures of 100°–200°C and subsequent devolatilization of the polymer for removal of residual monomer at 200°–225°C. Hui and Hamielec¹ made a comprehensive experimental investigation of the kinetics of bulk thermal polymerization of styrene in the temperature range of 100°–200°C. Initiation third order with respect to monomer gave an adequate fit to rate and molecular weight data. The present work extends the kinetic study to temperatures of 200°–230°C and investigates the validity of their model at these elevated temperatures.

REACTION KINETICS

The basic mechanism outlined by Pryor and Lasswell² is given below.

Initiation



In the above scheme M is the monomer, $\dot{\text{R}}_1$ is a free radical with one monomer unit, and AH is a Diels-Alder adduct.

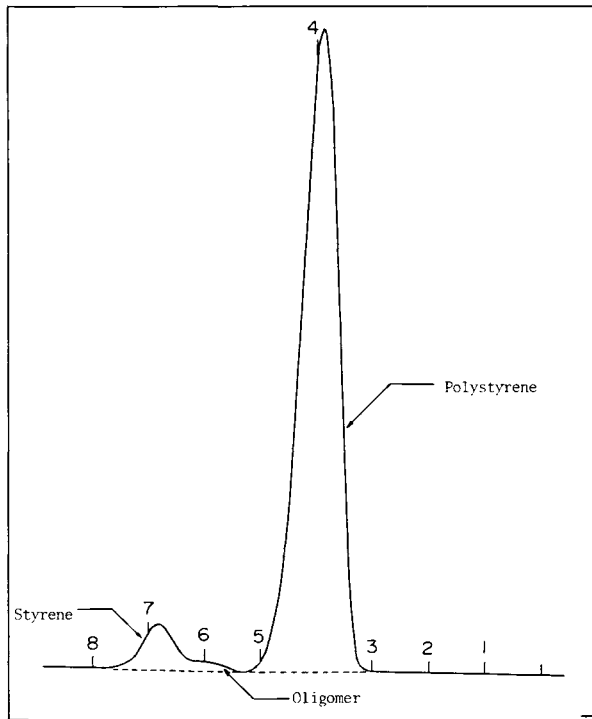


Fig. 1. GPC analysis. Sample, polystyrene, 200°C, 60 min, not degassed; solvent, tetrahydrofuran; sensitivity, 2X; concentration, 0.25 wt-%; flow rate, 1–2 cc/min; temperature, room; column specification, Microstyrigel (one 500 Å and two 100 Å columns).

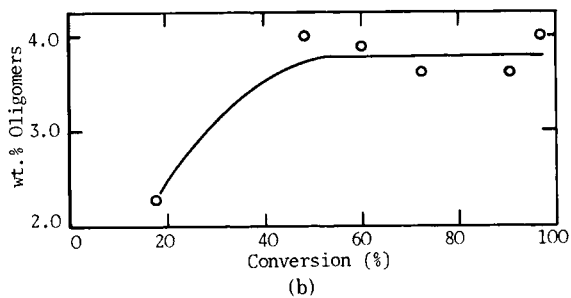
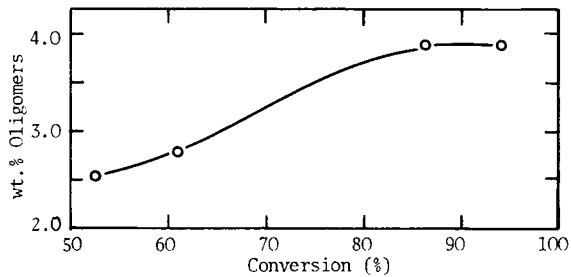


Fig. 2. (a) Oligomeric content at 200°C; (b) oligomeric content at 220°C.

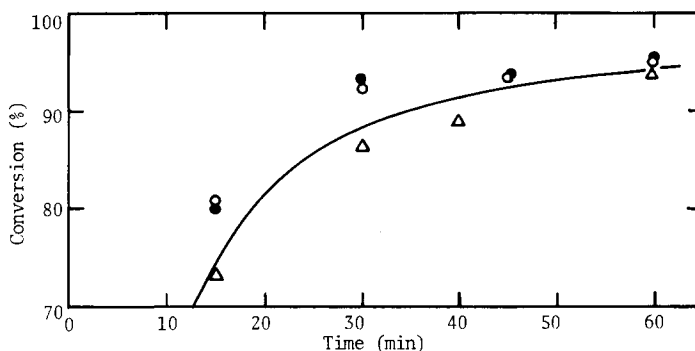


Fig. 3. Conversion history at 200°C: (○) present data (monomer degassed); (●) present data (monomer not degassed); (Δ) Hui's data; (—) prediction (Hui's model).

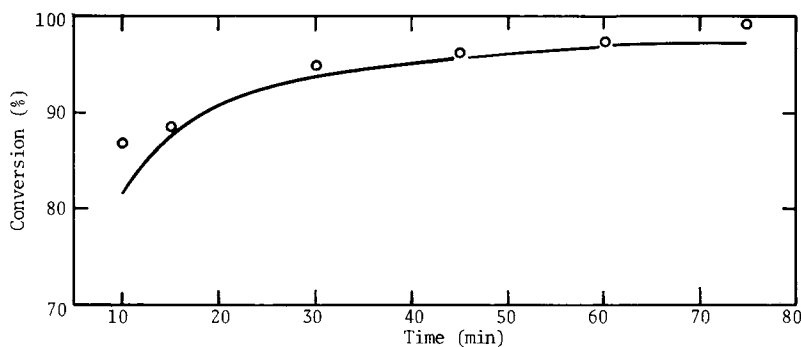


Fig. 4. Conversion history at 220°C: (○) present data (monomer not degassed); (—) prediction (Hui's model).

Propagation



Termination by Combination



Chain Transfer



where P_r is a polymer molecule with r monomer units. Termination by disproportionation is negligible in polymerization of styrene. Chain transfer occurs mainly to AH.

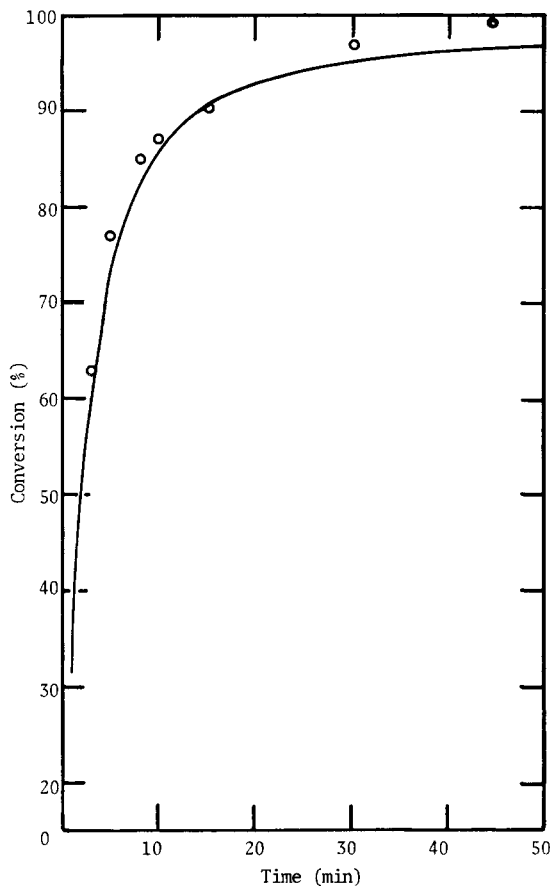


Fig. 5. Conversion history at 230°C: (O) present data (monomer not degassed); (—) prediction (Hui's model).

MATHEMATICAL MODEL

In deriving the model, the stationary-state hypothesis (SSH) and the long-chain hypothesis (LCH) are assumed valid. Diffusion-controlled termination reactions are accounted for using an empirical fit of k_t versus conversion.

Thermal Initiation

Using the initiation scheme outlined above, eqs. (1a)–(1e), the initiation rate has been shown¹ to be

$$I = \frac{2k_i k_1 [M]^3}{k_{-1} + (k_i + k_c)[M] + k_{fAH} \left[\left(\frac{I}{k_t} \right)^{1/2} \right]} \quad (5)$$

When

$$k_{-1} \gg (k_i + k_c)[M] + k_{fAH} \left[\left(\frac{I}{k_t} \right)^{1/2} \right]$$

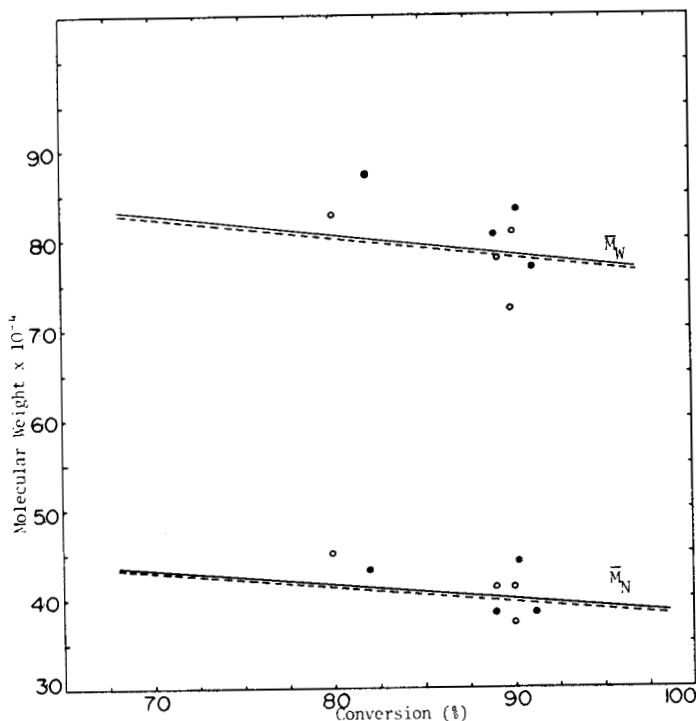


Fig. 6. Molecular weight averages at 200°C: (●) present data (monomer degassed); (○) present data (monomer not degassed); (—) prediction (Hui's model); (- - -) prediction (Hui's model with refitted B_1).

eq. (5) reduces to

$$I = \left(\frac{2k_i k_1}{k_{-1}} \right) [M]^3 = 2\bar{k}_i [M]^3 \quad (6)$$

Rate Expression

To account for the significant volume shrinkage which occurs in the polymerization of styrene, a variable volume equation is used:

$$R_p = -\frac{1}{V} \frac{dN}{dt} = -\frac{1}{V} \frac{d}{dt} ([M]V) \quad (7a)$$

$$\frac{d[M]}{dt} = -R_p - \frac{[M]}{V} \frac{dV}{dt} \quad (7b)$$

$$\frac{d[M]}{dt} = -k_p [M] \left[\left(\frac{I}{k_t} \right)^{1/2} \right] \frac{[M]}{V} \frac{dV}{dt} \quad (7c)$$

Assuming volume to vary linearly with conversion,

$$V = V_0(1 + \epsilon x) \quad (8a)$$

where

$$\epsilon = \frac{(V)_{x=1} - (V)_0}{(V)_0} \quad (8b)$$

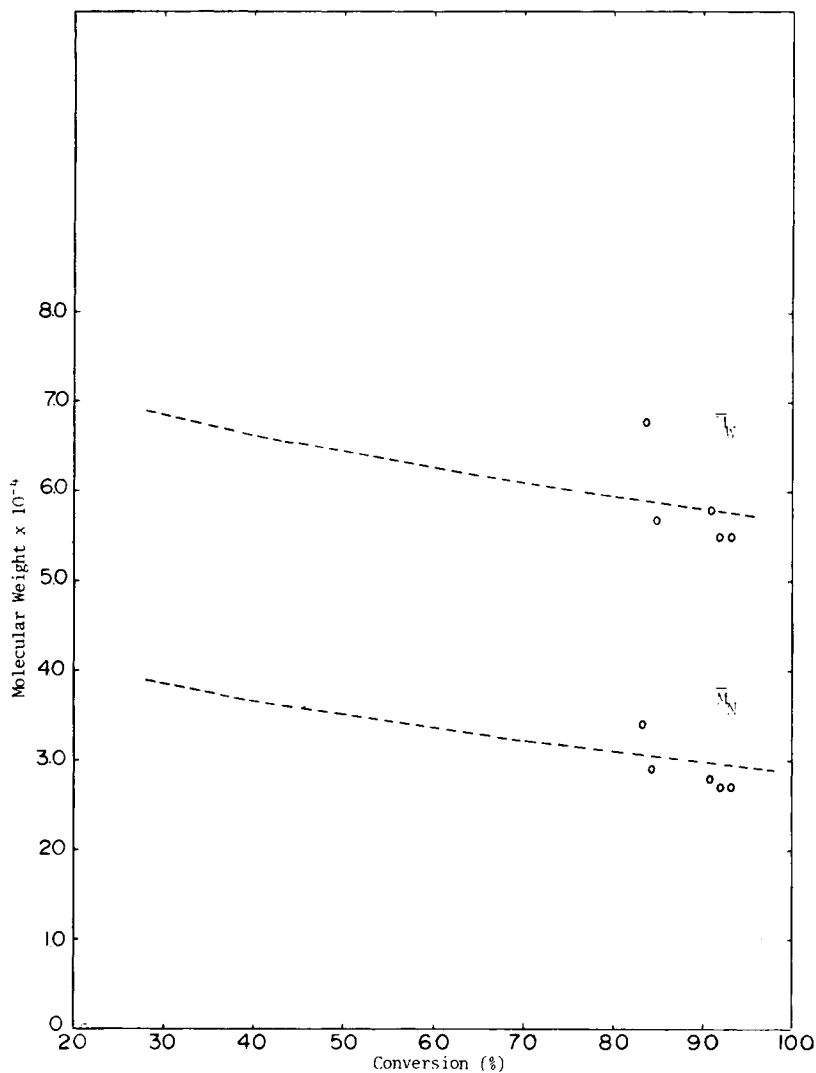


Fig. 7. Molecular weight averages at 220°C: (O) present data (monomer not degassed); (---) prediction (Hui's model with refitted B_1).

$$x = \frac{[M]_0 V_0 - [M] V}{[M]_0 V_0} \quad (8c)$$

From eqs. (8a)–(8c),

$$x = \frac{[M]_0 - [M]}{[M]_0 + [M]\epsilon} \quad (8d)$$

Also,

$$\frac{1}{V} \frac{dV}{dt} = - \left(\frac{\epsilon}{[M]_0 + \epsilon[M]} \right) \frac{d[M]}{dt} \quad (8e)$$

Substituting eq. (8e) in eq. (7c) and simplifying gives

$$\frac{d[M]}{dt} = -k_p [M] \left[\left(\frac{I}{k_t} \right)^{1/2} \right] \left(\frac{[M]_0 + \epsilon[M]}{[M]_0} \right) \quad (9)$$

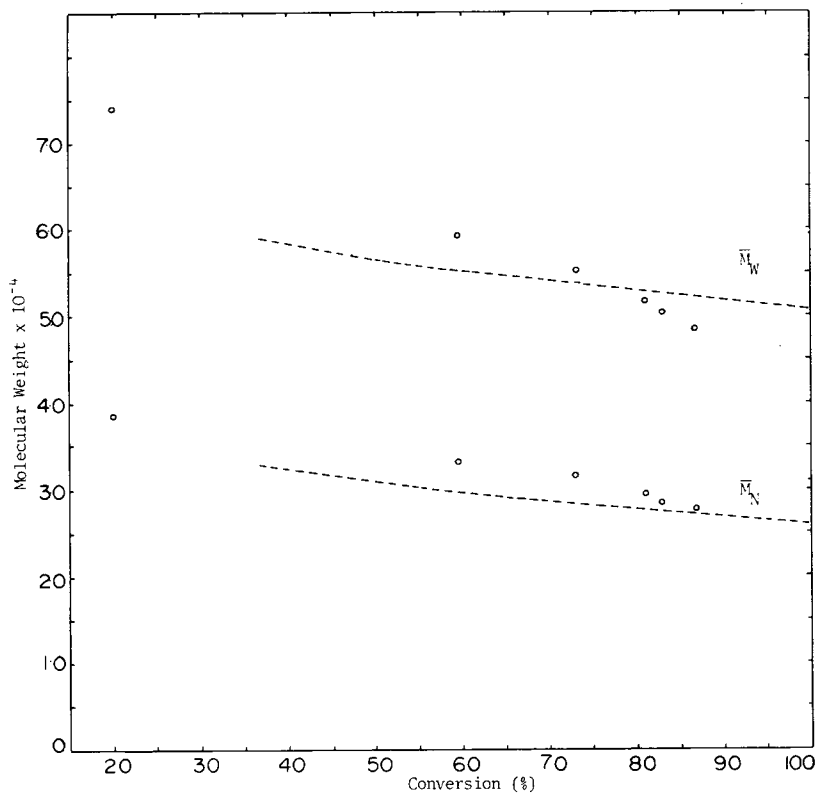


Fig. 8. Molecular weight averages at 230°C: (O) present data (monomer not degassed); (- - -) prediction (Hui's model with refitted B_1).

The conversion history is obtained by solving eqs. (9) and (8d).

Chain Length Averages and Chain Length Distributions

The instantaneous chain length distribution and chain length averages are given by

$$W(r)_{\text{inst}} = (\tau + \beta)[\tau + \frac{1}{2}\beta(\tau + \beta)r]r \exp\{-(\tau + \beta)r\} \quad (10)$$

$$\bar{r}_{N_{\text{inst}}} = \frac{1}{(\tau + \beta/2)} \quad (11)$$

$$\bar{r}_{W_{\text{inst}}} = \frac{2\left(\tau + \frac{3}{2}\beta\right)}{(\tau + \beta)^2} \quad (12)$$

where

$$\tau = \frac{k_{fm}}{k_p} \quad (13)$$

$$\beta = \frac{k_t R_p}{k_p^2 [M]^2} \quad (14)$$

It should be noted that according to Hui and Hamielec,¹ the effect of transfer to AH is accounted for in this analysis by employing an effective τ .

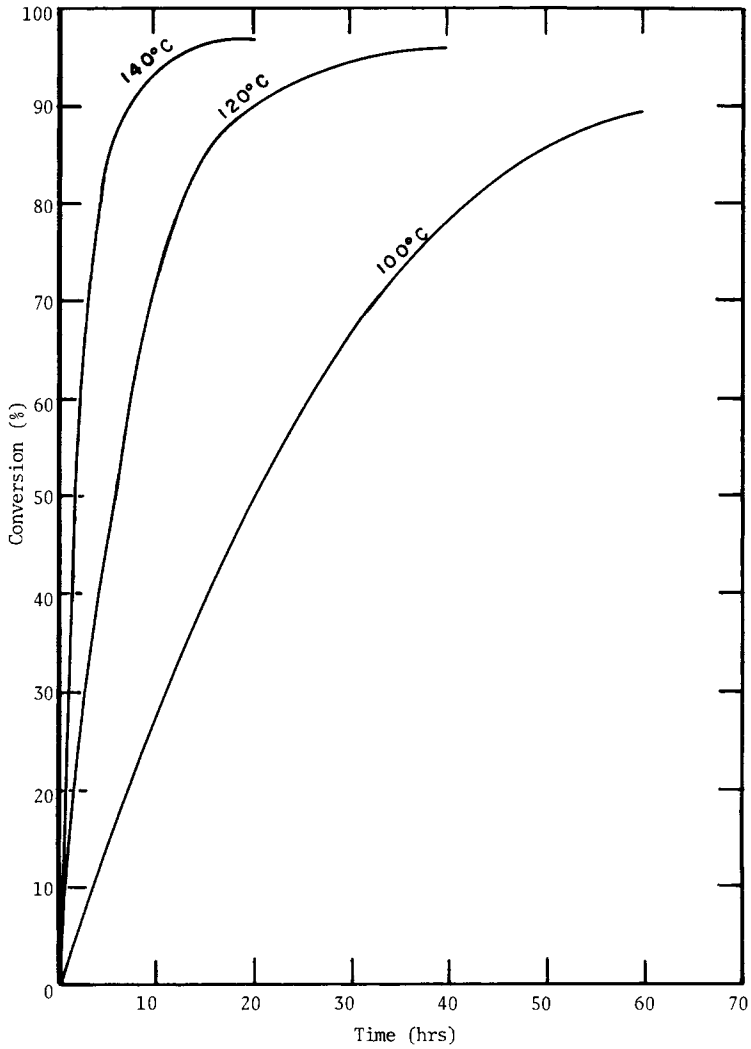


Fig. 9. Model prediction of conversions.

The cumulative chain length distribution and chain length averages are given by

$$W(r)_{\text{cum}} = \frac{1}{x} \int_0^x W(r)_{\text{inst}} dx \quad (15)$$

$$\frac{1}{\bar{r}_{N_{\text{cum}}}} = \frac{1}{x} \int_0^x \frac{1}{\bar{r}_{N_{\text{inst}}}} dx \quad (16)$$

$$\bar{r}_{W_{\text{cum}}} = \frac{1}{x} \int_0^x \bar{r}_{W_{\text{inst}}} dx \quad (17)$$

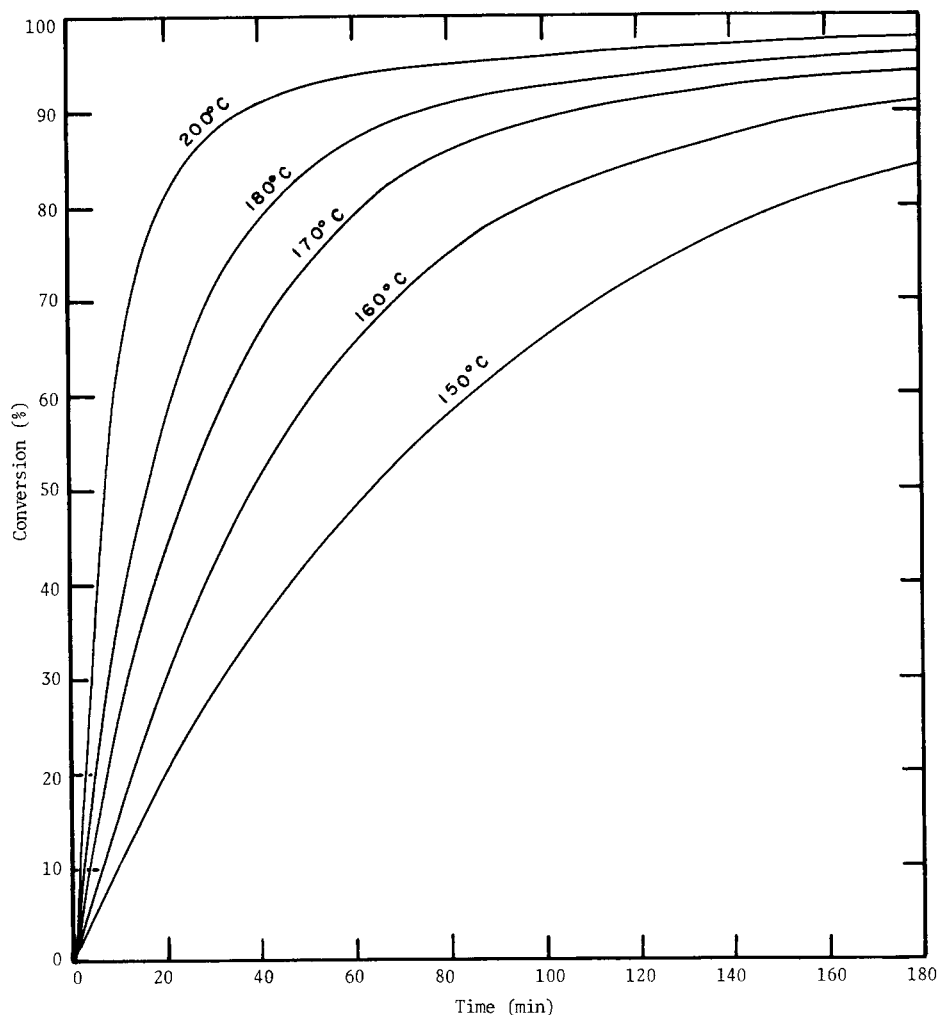


Fig. 10. Model prediction of conversions (cont.).

Diffusion-Controlled Kinetics

Hui and Hamielec¹ accounted for diffusion-controlled termination by fitting the following group of parameters to their experimental data:

$$A = \left(\frac{2\bar{k}_i}{k_t/k_p^2} \right)^{1/2} \quad (18)$$

$$A = A_0 \exp(A_1x + A_2x^2 + A_3x^3) \quad (19)$$

where for any temperature \bar{k}_i , A_0 , A_1 , A_2 , A_3 , and B_1 are independent of conversion:

$$\frac{k_{fm}}{k_p} = \left(\frac{k_{fm}}{k_p} \right)_0 + B_1x \quad (20)$$

In eq. (20) the second term is used to correct for transfer to by-products of initiation (such as AH) giving an effective transfer to monomer constant. The importance of transfer to by-products has been reported by Pryor and Coco³ who

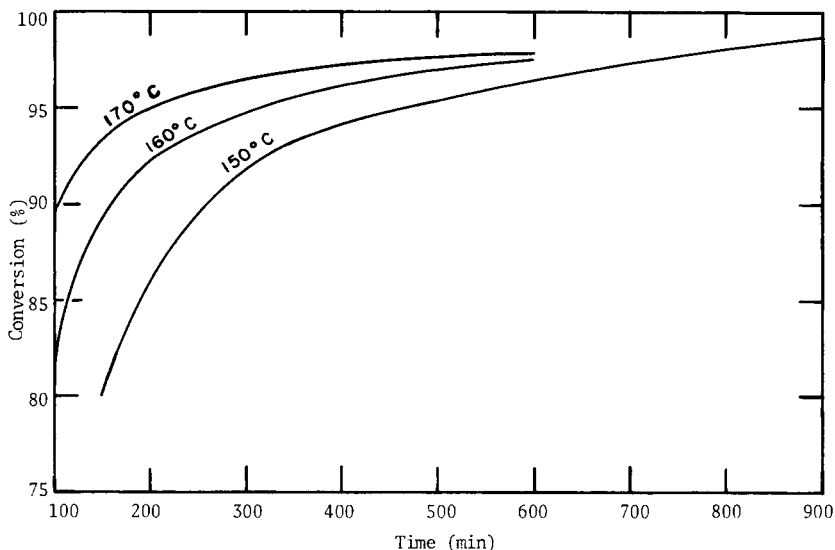


Fig. 11. Model prediction of conversions (cont.).

state that a large portion of the previously reported transfer constant of styrene is actually the result of transfer to AH:

$$\left(\frac{k_{fm}}{k_p}\right)_{\text{apparent}} = \left(\frac{k_{fm}}{k_p}\right)_{\text{styrene}} + \left(\frac{k_{fAH}}{k_p}\right) \frac{[AH]}{[M]} \quad (21)$$

Equation (20) is an empirical form of eq. (21). In the present study experimental conversions and molecular weight averages were fitted using eqs. (18)–(20). The rate constants at the initial condition of zero conversion are as follows⁴:

$$(k_p)_0 = 1.051 \times 10^7 \exp(-3557/T) \quad (22)$$

$$(k_{fm})_0 = 2.31 \times 10^6 \exp(-6377/T) \quad (23)$$

$$(k_t)_0 = 1.255 \times 10^9 \exp(-844/T) \quad (24)$$

Densities of styrene monomer and polystyrene⁵ used in the model are

$$\rho_m = 924 - 0.918(T - 273.1) \quad (25)$$

$$\rho_p = 1084.8 - 0.605(T - 273.1) \quad \text{in g/l.} \quad (26)$$

EXPERIMENTAL

Experiments were performed in bulk in sealed glass ampoules (5 and 10 mm O.D.). Temperatures investigated were 200°, 220°, and 230°C. Polymerizations were performed both in presence and in absence of air. Uninhibited styrene was used. Details of the experimental technique may be found elsewhere.⁶

Monomer conversions and polymer molecular weight distributions were measured by gel permeation chromatography. Molecular weight averages calculated from the chromatograms were corrected for axial dispersion and skewing. Figure 1 illustrates a typical chromatogram obtained in the study. In addition to the monomer and polymer peak, it indicates the presence of oligomers. The conversions evaluated by dividing the area under the polystyrene peak by the

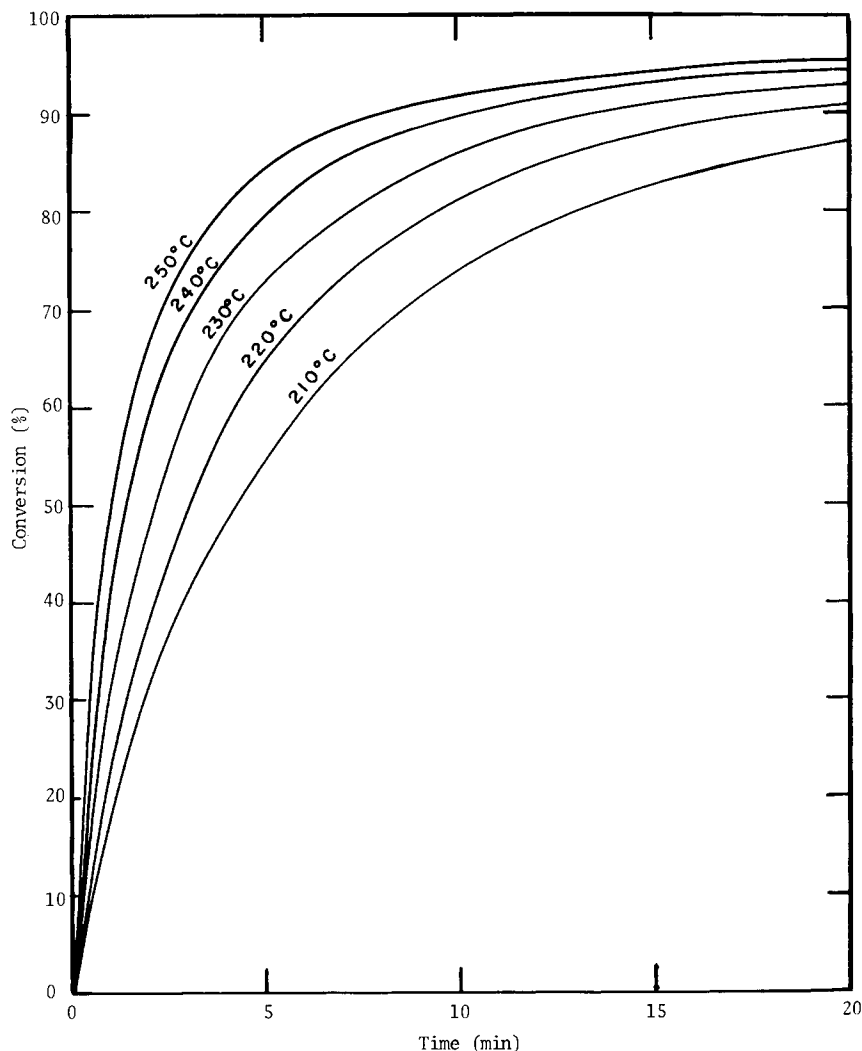


Fig. 12. Model prediction of conversions (cont.).

total area under the chromatogram were corrected using Figure 2 to account for the conversion of monomer to oligomers. The results shown in Figure 2 were obtained from an unpublished study conducted to determine the weight percentage of oligomers in the polymerization mixture for isothermal thermally initiated bulk polymerization at 200° and 220°C.⁷ The weight percentage of oligomers were measured by GPC from three separate peaks (one for monomer, one for polymer, and one for the oligomers).

RESULTS AND DISCUSSION

The experimental rate and molecular weight data are shown in Figures 3–8. As shown in Figures 3 and 6, there is no significant difference between the rates and molecular weights obtained for degassed and nondegassed monomer. This

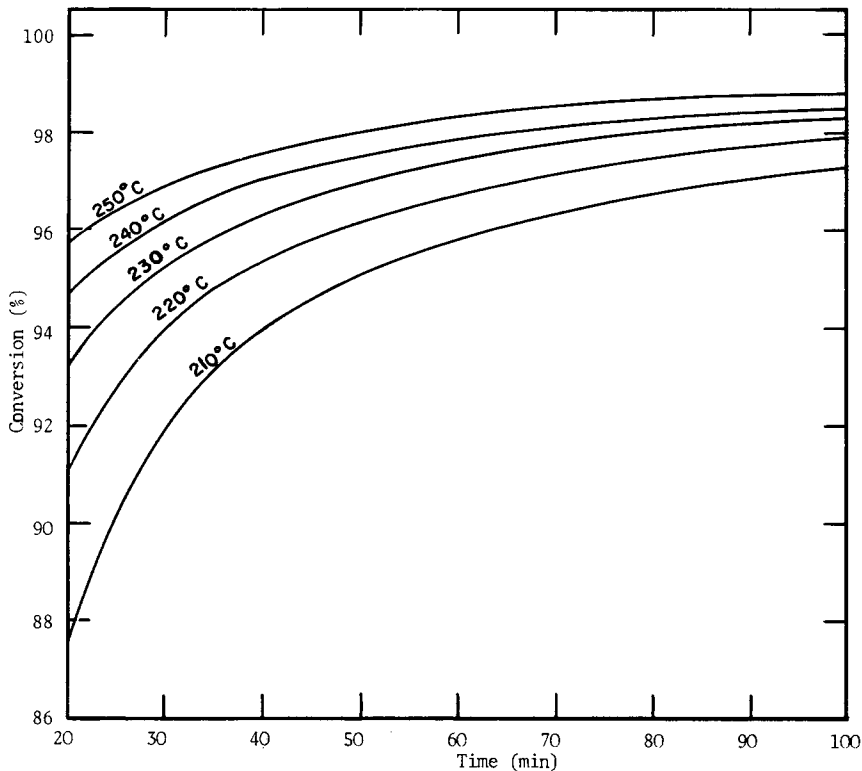


Fig. 13. Model prediction of conversions (cont.)

observation has implications for commercial practice where a nitrogen blanket is often employed.

The molecular weight data shown in Figures 6–8 indicate that the molecular weights are relatively constant with conversion. Polydispersity ratios obtained are close to 2.0, implying that a polymer with the most probable distribution is obtained. This suggests that the molecular weight development is controlled by transfer reactions.

Also shown in Figures 3–8 are the model predictions. The model parameters estimated by Hui and Hamielec¹ are given as

$$A_0 = 1.964 \times 10^5 \exp(-10,040/T) \quad (27)$$

$$A_1 = 2.57 - 5.05 \times 10^{-3}T \quad (28)$$

$$A_2 = 9.56 - 1.76 \times 10^{-2}T \quad (29)$$

$$A_3 = -3.03 + 7.85 \times 10^{-3}T \quad (30)$$

$$B_1 = -1.013 \times 10^{-3} \log_{10} \left(\frac{473.12 - T}{202.5} \right) \quad (31)$$

$$\bar{k}_i = 2.19 \times 10^5 \exp(-13810/T) \quad \text{in l.}^2/(\text{g-mole}^2 \text{ sec}) \quad (32)$$

where T is in °K.

Since eq. (31) cannot be solved for temperatures exceeding 200°C, the pa-

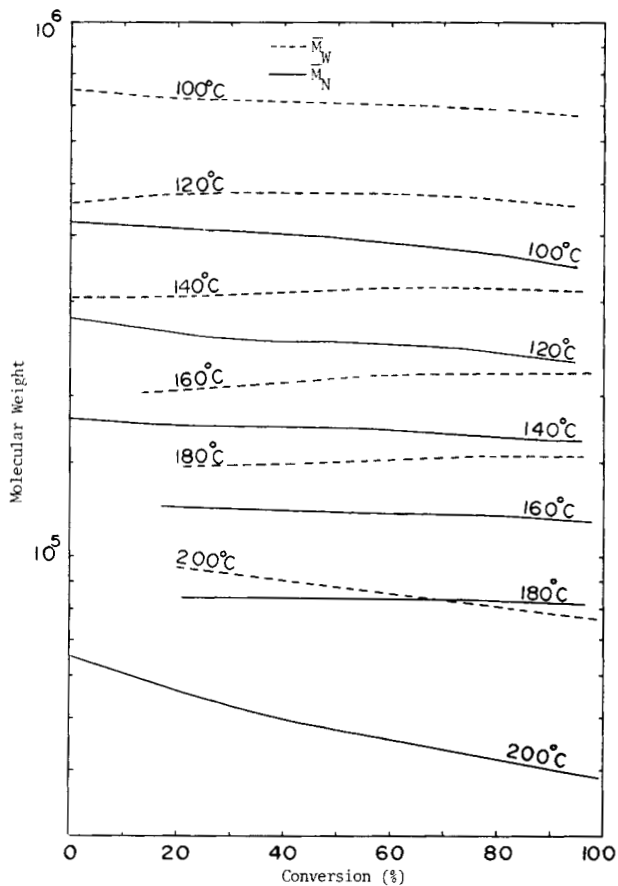


Fig. 14. Model prediction of molecular weight (cont.).

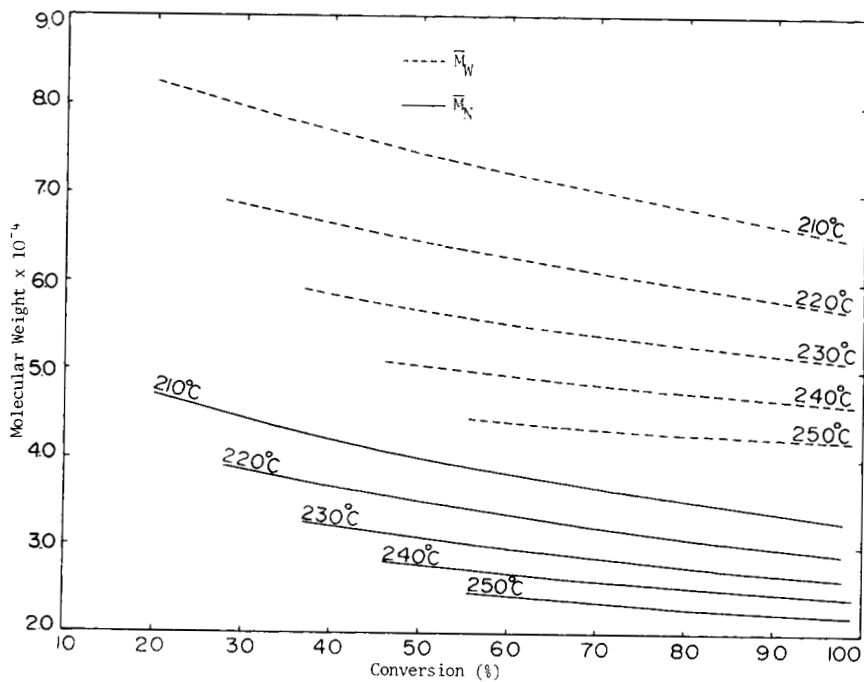


Fig. 15. Model prediction of molecular weights (cont.).

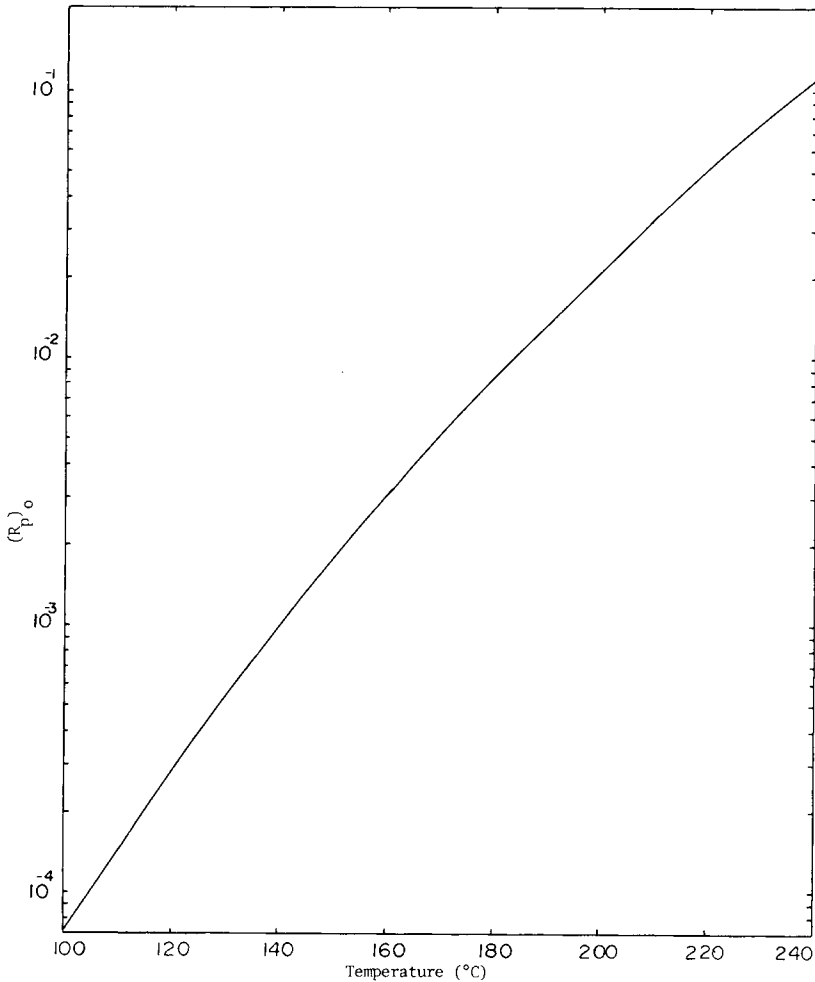


Fig. 16. Variation of initial rate at zero conversion with temperature.

parameter B_1 was refitted using present molecular weight data by minimizing the objective function F given by

$$F = (M_{N_{\text{calcd}}} - M_{N_{\text{exper}}})^2 + (M_{W_{\text{calcd}}} - M_{W_{\text{exper}}})^2 \quad (33)$$

The refitted B_1 is given as

$$B_1 = \frac{10^{-2}E_1}{1 + 2E_1} \quad (34)$$

where

$$E_1 = 0.9755 \exp \left[-12180 \left(\frac{1}{T} - \frac{1}{473} \right) \right] \quad (35)$$

where T is in °K. Equations (34) and (35) are recommended for use at temperatures of 200°C and above.

As shown in Figure 3, the conversion-time data measured in this study by GPC tend to be higher than the data obtained by Hui.¹ Hui measured conversions gravimetrically and by UV spectrophotometry. Both methods fail to completely

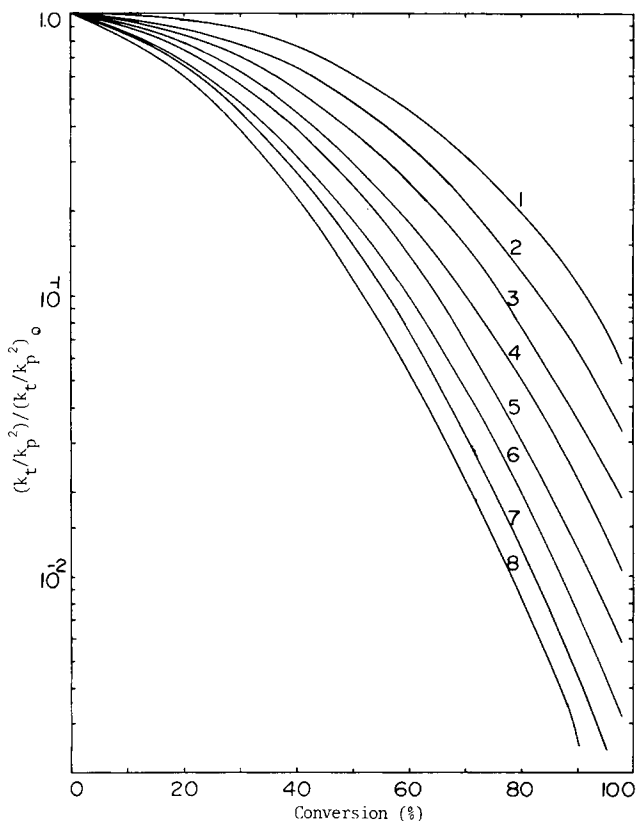


Fig. 17. Variation of $(k_t/k_p^2)/(k_t/K_p^2)_0$ with conversion: (1) 240°C; (2) 220°C; (3) 200°C; (4) 180°C; (5) 160°C; (6) 140°C; (7) 120°C; (8) 100°C.

account for the presence of oligomers, the former because of incomplete precipitation and the latter because the absorption by oligomer species is uncertain. For the same reason, model prediction of conversions (Figs. 3–5) tend to be lower than experimental data. However, the agreement at 220° and 230°C is fairly close. Molecular weight predictions agree reasonably well with the experimental data (Figs. 6–8) for all temperatures.

The model was used to generate conversion-versus-time and molecular weight-versus-conversion curves for temperatures ranging from 100° to 250°C (Figs. 9–15). The molecular weights between 100° and 180°C were fitted versus conversion and temperature. The fits are given by

$$\bar{M}_W = [C_1 + C_2(x - 0.5)] \times 10^5 \quad (36)$$

$$\bar{M}_N = [C_3 + C_4(x - 0.5)] \times 10^5 \quad (37)$$

where

$$C_1 = 2.282 \times 10^6 T^{-2.747} \quad (38)$$

$$C_2 = -\left(1 + \frac{T}{42.1}\right) \exp\left(\frac{-T}{42.1}\right) \quad (39)$$

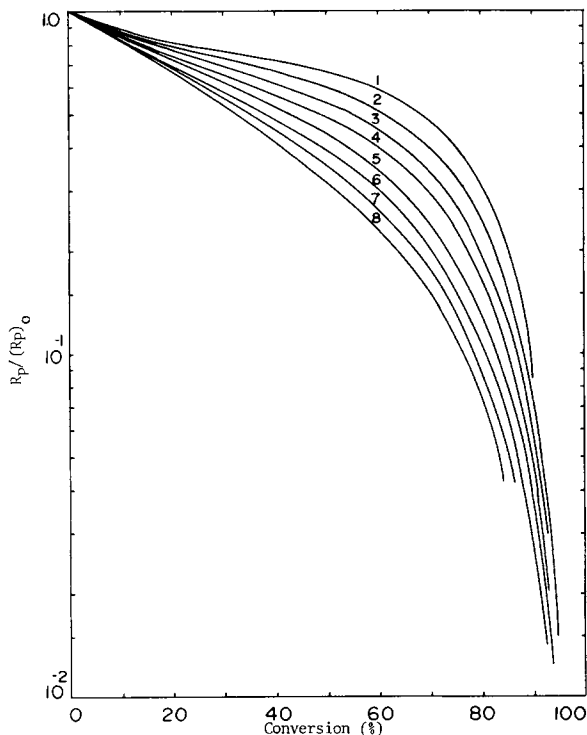


Fig. 18. Variation of $R_p/(R_p)_0$ with conversion: (1) 100°C; (2) 120°C; (3) 140°C; (4) 160°C; (5) 180°C; (6) 200°C; (7) 220°C; (8) 240°C.

$$C_3 = 0.9324 \times 10^6 T^{-2.69} \quad (40)$$

$$C_4 = -\left(1 + \frac{T}{58.25}\right) \exp\left(\frac{-T}{58.25}\right) \quad (41)$$

where equations (36) and (37) permit the evaluation of molecular weight averages without actually solving the model equations. They are recommended for performing approximate estimates of the molecular weights for any given temperature and conversion.

The dramatic reduction with conversion of the group of rate constants k_t/k_p^2 is shown in Figure 17. Figure 18 shows the fall in rate with conversion for temperatures of 100° to 240°C predicted by the model. The initial rate at zero conversion is shown as a function of temperature in Figure 16. At 100°C for a conversion of 20%, $R_p/(R_p)_0$ is 0.81, while $(k_t/k_p^2)/(k_t/k_p^2)_0$ is 0.6, the corresponding values at 240°C being 0.66 and 0.94, respectively. The model thus predicts a much less severe gel effect at 240°C than at 100°C, a lower $R_p/(R_p)_0$ at 240°C being the consequence.

In conclusion, it may be said that the model developed by Hui and Hamielec¹ appears to be useful for temperatures up to 230°C. Calculated conversion histories and molecular weights are reported herein over a wide range of temperatures, 100°–250°C (of interest in commercial polystyrene production), in a form easy to apply and suitable for ready reference.

Nomenclature

I	rate of initiation, g-mole/(l. sec)
k_{fAH}	rate constant for chain transfer to AH, l./(g-mole sec)
k_{fm}	rate constant for chain transfer to monomer M, l./(g-mole sec)
\bar{k}_i	rate constant for thermal initiation, l. ² /(g-mole ² sec)
\bar{k}_p	rate constant for propagation, l./(g-mole sec)
\bar{k}_t	rate constant for termination, l./(g-mole sec)
\bar{M}	monomer molecular weight
N	total number of moles, g-moles
\bar{r}_N	number-average chain length ($\bar{M}_N = \bar{M}\bar{r}_N$)
\bar{r}_W	weight-average chain length ($\bar{M}_W = \bar{M}\bar{r}_W$)
R_p	rate of polymerization, g-mole/(l. sec)
t	time, sec
T	temperature, °C or °K
V	volume, l.
$W(r)$	weight fraction of chain length r
x	monomer conversion
ρ	density, g/l.

Subscript

0 refers to initial condition (zero conversion)

References

1. A. W. Hui and A. E. Hamielec, *J. Appl. Polym. Sci.*, **16**, 749 (1972).
2. W. A. Pryor and L. D. Lasswell, in *Advances in Free Radical Chemistry*, Vol. 5, G. H. Williams, Ed., Elek Science, London, 1975.
3. W. A. Pryor and J. H. Coco, *Macromolecules*, **3**, 500 (1970).
4. J. H. Duerksen, A. E. Hamielec, and J. W. Hodgins, *A.I.Ch.E. J.*, **13**, 1081 (1967).
5. W. Patnode and W. J. Scheiber, *J. Am. Chem. Soc.*, **61**, 3449 (1939).
6. A.W. Hui, Ph.D. Thesis, McMaster University, Hamilton, Canada, 1970.
7. A. E. Hamielec, unpublished data, 1975.

Received February 2, 1977